Chimica Techno Acta
published by Ural Federal University
eISSN 2411-1414; chimicatechnoacta.ru

ARTICLE
2022, vol. 9(2), No. 20229205
DOI: 10.15826/chimtech.2022.9.2.05

# Synthesis and luminescent properties of new double $Ln_2Zr(WO_4)_5$ (Ln = Tb, Dy) tungstates

Bair Bazarov [a,b*], Sesegma G. Dorzhieva [a], Roman Yu. Shendrik [c,d], Yunna L. Tushinova [a,b], Tsirendyzhit T. Bazarova [a], Dmitriy O. Sofich [c], Olga D. Chimitova [a], Jibzema G. Bazarova [a]

a: Baikal Institute of Nature Management SB RAS, Ulan-Ude 670047, Russia
b: Department of Inorganic and Organic Chemistry, Buryat State University, Ulan-Ude 670000, Russia
c: A.P. Vinogradov Institute of Geochemistry SB RAS, Irkutsk 664033, Russia
d: Irkutsk State University, Irkutsk 664033, Russia
* Corresponding author: info@binm.ru; bazbg@rambler.ru

This paper belongs to a Regular Issue.



## Abstract

New polycrystalline powder samples of double $Ln_2Zr(WO_4)_5$ (Ln = Dy, Tb) tungstates were synthesized using high-temperature solid-phase and sol-gel methods. The conditions of the sol-gel synthesis of tungstates were optimized. The obtained phases were characterized by the X-ray powder diffraction on the basis of the crystallographic data of similar Ln–Zr molybdates. It is found that $Ln_2Zr(WO_4)_5$ (Ln = Dy, Tb) double tungstates crystallize in the orthorhombic crystal system, space group $Cmc2_1$ ($Z$ = 4). The intensive luminescence in the green spectral region for $Tb_2Zr(WO_4)_5$ and yellow spectral region for $Dy_2Zr(WO_4)_5$ was shown.

## Keywords

solid-phase synthesis
sol-gel technique
framework structure
luminescence
tungstates
lanthanides

Received: 08.11.21
Revised: 19.04.22
Accepted: 26.04.22
Available online: 03.05.22

## 1. Introduction

The search and synthesis of new compounds are associated with the study of multicomponent systems. In terms of the formation of promising compounds, molybdate and tungstate systems are of great interest [1–19]. Complex oxide compounds containing REE and elements of the IV B subgroup (Ti, Zr, Hf) are the objects of intensive research in connection with the search of new materials used as solid-state electrolytes, phosphors and matrices for immobilizing radioactive waste. Previously, we studied interactions in the ternary oxide systems in the subsolidus region by the intersecting cuts method and established the formation of three types of compounds with following formulas: $Ln_2Zr_3(MoO_4)_9$ (1:3) (Ln = La–Tb), $Ln_2Zr_2(MoO_4)_7$ (1:2) (Ln = Sm–Dy), $Ln_2Zr(MoO_4)_5$ (1:1) (Ln = Tb–Lu) [20–22]. The crystal structures for the double molybdate representatives were also studied [23]. This work was devoted to synthesis and luminescent characteristics of double tungstates $Ln_2Zr(WO_4)_5$ (Ln = Tb, Dy) obtained by a solid-phase synthesis and sol-gel methods. It was established that the tungstate phases are isostructural to the molybdenum analogues.

## 2. Experimental

New $Ln_2Zr(WO_4)_5$ (Ln = Tb, Dy) tungstates were obtained by the solid-phase reaction and sol-gel technique. For solid-phase synthesis, $Ln_2O_3$ (99.9% purity), $ZrO_2$ obtained by calcining $ZrO(NO_3)_2{\cdot}2H_2O$ (analytical grade), $WO_3$ (analytical grade) were used as starting reagents. The initial oxides, preliminary calcined at T=200 °C, were thoroughly mixed in appropriate ratios. The samples were annealed in porcelain crucibles in air in a muffle furnace. The initial annealing temperature was 450 °C. The final synthesis temperature was varied in the range of 750–800 °C with 50 h dwell time. In the course of synthesis, the samples were repeatedly ground in an agate mortar in ethanol. The phases were identified by X-ray phase analysis using a D8 Advance Bruker diffractometer.

Also, double tungstates $Ln_2Zr(WO_4)_5$ (Ln = Tb, Dy) were synthesized by the Pechini method, where ethylene glycol is completely replaced by water, there by reducing the amount of organic compounds. The second difference is the formation of an amorphous gel-like substance instead of a polymer. As a complexing agent, as in the Pechini method, an aqueous solution of citric acid ($C_6H_8O_7{\cdot}H_2O$) was used.

The excitation and emission spectra in the UV-IR range were measured using a MDR-2 laboratory monochromator and a SDL-1 dual monochromator. The absorption spectra were obtained using a Perkin-Elmer Lambda 950 UV/VIS/NIR spectrophotometer, operating in the range of 180–3000 nm with a maximum resolution of 0.2 nm. To measure the absorption spectra of powder samples to the device, a prefix was connected to the integrating sphere with a diameter of 150 mm. Powder was poured into a quartz ampoule and was fixed in the holder of the integrating sphere. The absorption of the test glass was subtracted from the absorption spectra.

## 3. Results and Discussion

$Ln_2Zr(WO_4)_5$ (Ln = Tb, Dy) double tungstates were obtained by ceramic and sol-gel methods. The conditions of the sol-gel technique for obtaining of $Ln_2Zr(WO_4)_5$ (Ln = Tb, Dy) were optimized. The synthesis scheme is shown in Figure 1.

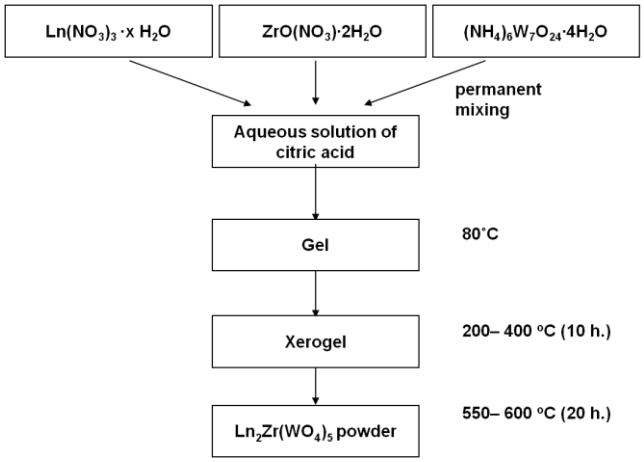


**Figure 1** Block diagram of the sol-gel technique for obtaining of $Ln_2Zr(WO_4)_5$ (Ln = Tb, Dy) tungstates.

According to the X-ray powder diffraction data, all compounds synthesized by two methods are isostructural. Crystallographic parameters of double tungstates was determined using the TOPAZ 4.2 program according to data of isostructural high-temperature phase of $Er_2Zr(MoO_4)_5$ molybdate [24]. The results of refinement are shown in Table 1. $Ln_2Zr(WO_4)_5$ (Ln = Tb, Dy) are crystallized in orthorhombic crystal system, space group $Cmc2_1$ ($Z$ = 4). The shape and intensity of the spectral lines indicate low symmetry of rare-earth ions coordination, which is in good agreement with the crystallographic data of molybdates. As an example, Figure 2 shows an X-ray diffraction pattern for $Tb_2Zr(WO4)_5$ obtained by the solid state reaction.

**Table 1** The refinement parameters for $Ln_2Zr(WO_4)_5$ (Ln = Tb, Dy).

| Empirical formula | $Tb_2Zr(WO4)5$ | $Dy_2Zr(WO_4)_5$ |
|---|---|---|
| Formula weight, g/mol | 1648.31 | 1655.46 |
| Crystal system | Orthorhombic | |
| Space group | $Cmc2_1$ | |
| Cell parameters, Å | $a$ = 21.078(1)<br>$b$ = 9.6844(4)<br>$c$ = 9.8164(6) | $a$ = 21.177(1)<br>$b$ = 9.6737(7)<br>$c$ = 9.8176(8) |
| Cell volume, Å$^3$ | 2003.8(1) | 2011.3(2) |
| $Z$ | 4 | |
| Calc. density, g/sm$^3$ | 4.061 | 4.047 |
| $R_{wp}$, % | 2.88 | 6.75 |
| $R_p$, % | 2.24 | 5.34 |
| GOF | 1.80 | 1.21 |

The crystal structure of the studied tungstates can be represented by a three-dimensional mixed framework consisting of three polyhedra: $WO_4$ tetrahedra, Ln(2)/$ZrO_6$ octahedra and eight vertex polyhedra $Ln(1)O_8$ connected to each other through common oxygen atoms (Figure 3). Ln and Zr atoms are distributed with equal probability over equivalent crystallographic positions.

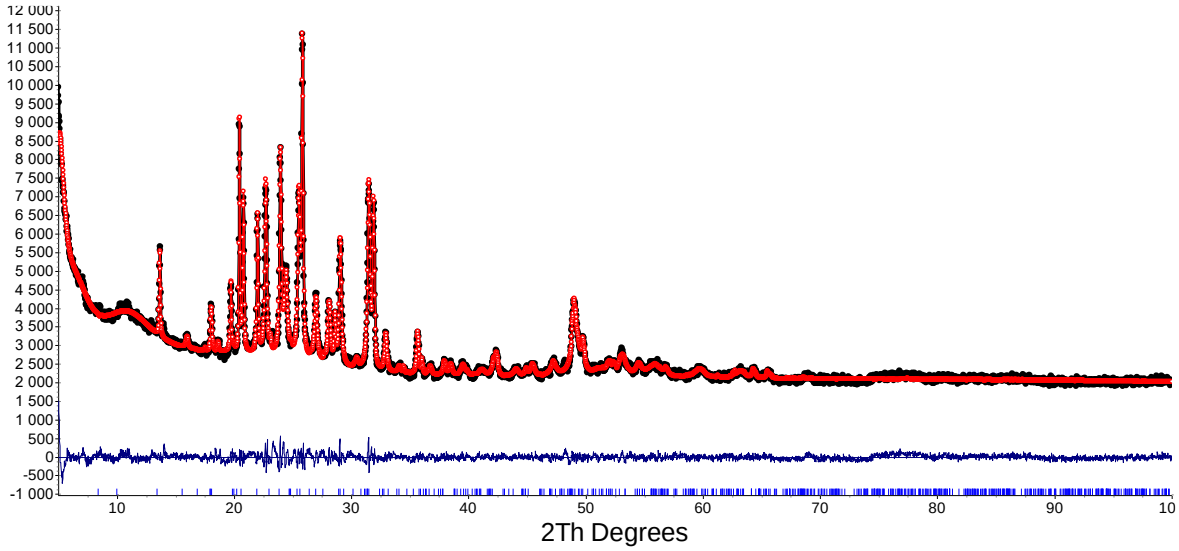


**Figure 2** Measured and calculated powder diffraction patterns for $Tb_2Zr(WO_4)_5$ together with the difference curve (Cu Kα1 radiation).

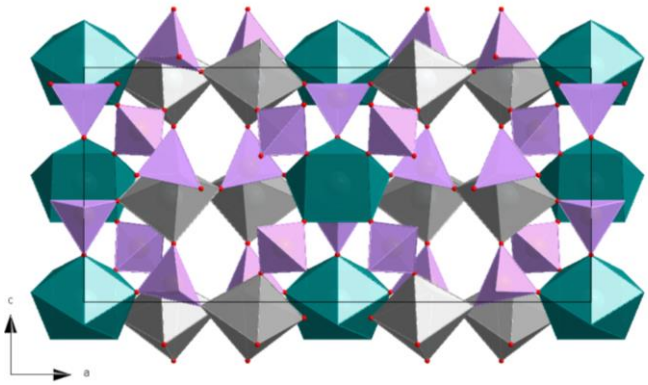

**Figure 3** The structural model of $Ln_2Zr(WO_4)_5$ (Ln = Tb, Dy), viewed along the *b* axis. Light-lilac tetrahedra are formed by W atoms, dark-grey octahedra by Ln(2)/Zr atoms and turquoise polyhedra by Ln(1)atoms.

In the excitation spectra of the investigated tungstates $Tb_2Zr(WO_4)_5$, two types of bands are observed – narrow, corresponding to transitions inside 4*f* shells of REE (rare earth elements) and broad bands associated with charge transfer bands in complexes $WO_4^{2-}$ on REE. The luminescence and excitation spectra of $Tb_2Zr(WO_4)_5$ in the band with an energy of 26500 $cm^{-1}$ (λ = 377 nm) are shown in Figure 4. The position of the bands associated with transitions inside the 4*f* shell remains almost unchanged in the molybdate and the tungstate. The vertical lines in Figure 4 represent the energies of corresponding terms according to Carnall [25].

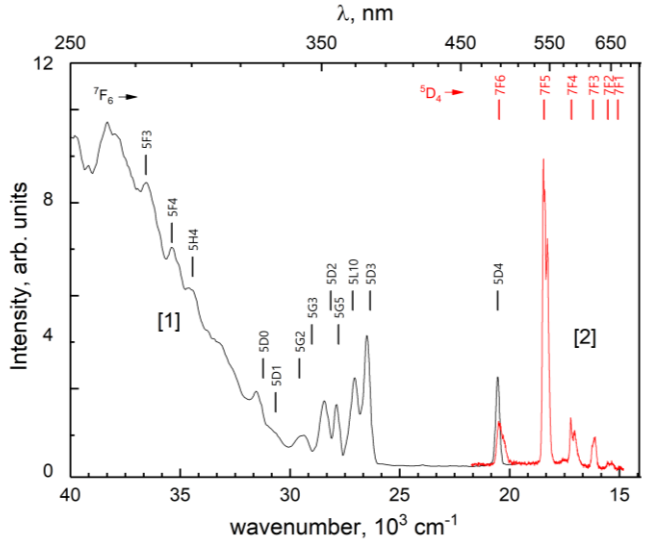


**Figure 4** Excitation (1) and luminescence (2) spectra of $Tb_2Zr(WO_4)_5$ tungstate.

Since $Tb_2Zr(WO_4)_5$ is isostructural to the corresponding molybdate analogue $Tb_2Zr(MoO_4)_5$ [26], all their spectra (luminescence, excitation) are similar. The luminescence spectra are characterized by the band with a highest intensity and maximum in the region of 18500 $cm^{-1}$ (λ = 540 nm) associated with the $^5D_4$–$^7F_5$ magnetic dipole transition. The luminescence band with a maximum at 20500 $cm^{-1}$ (λ = 488 nm) refers to the electric dipole transition $^5D_4$–$^7F_6$ in a $Tb^{3+}$ ion and depends on the symmetry of the crystal field; it is more intense than the other bands (except for $^5D_4$–$^7F_5$) and splits into three types, which indicates a spatial distortion of the 8-vertex $TbO_8$ polyhedra with a decrease in symmetry.

The absorption spectra of $Dy_2Zr(WO_4)_5$ (Figure 5) exhibit a number of bands corresponding to transitions from the ground term of the $^4F_{15/2}$ and 4*f*- state to higher energy terms. The position of the bands associated with transitions inside the 4*f* shell remains almost unchanged in the molybdate and in the tungstate.

Upon excitation by a laser with a wavelength of 404.5 nm, three emission bands with energies of 15100 $cm^{-1}$, 17400 $cm^{-1}$, and 20600 $cm^{-1}$ are observed (Figure 6, curve 2), associated with transitions inside the $Dy^{3+}$ ions. The most intense is the band with a maximum at 17400 $cm^{-1}$, associated with the transition from the $^4F_{9/2}$ term to the $^6H_{13/2}$ term (yellow region of the spectrum), the luminescence band at 20600 $cm^{-1}$ is associated with transitions from the $^4F_{9/2}$ to $^6H_{15/2}$ term (blue spectral region), and the 15100 $cm^{-1}$ band is associated with the $^4F_{9/2}$–$^6H_{11/2}$ transition (red spectral region).

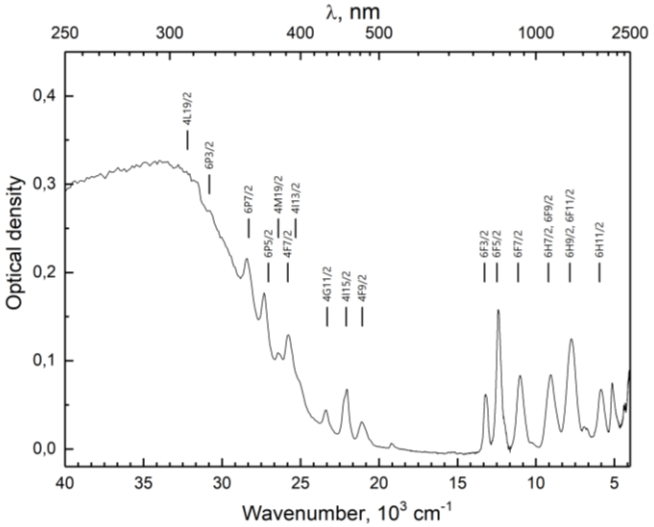


**Figure 5** Absorption spectrum of $Dy_2Zr(WO_4)_5$.

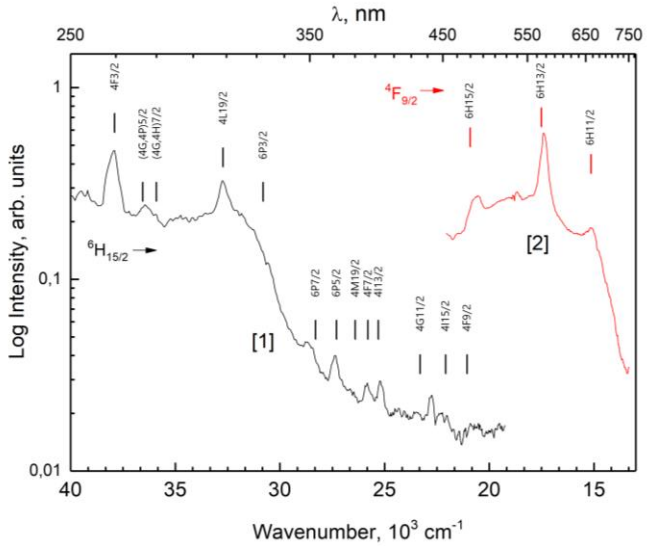


**Figure 6** Excitation (1) and emission (2) spectra of $Dy_2Zr(WO_4)_5$.

The $^4F_{9/2}$–$^6H_{15/2}$ transition is magnetic-dipole and its intensity weakly depends on the crystal environment. The $^4F_{9/2}$–$^6H_{13/2}$ transition is of the electric-dipole type. Due to low symmetry, the $^4F_{9/2}$–$^6H_{13/2}$ transition becomes partially allowed and its intensity is higher or comparable to the intensity of the $^4F_{9/2}$–$^6H_{15/2}$ transition in crystals without an inversion center. If a rare-earth ion occupies a position with an inversion center and its environment is sufficiently symmetric, then the transition intensity is significantly lower than $^4F_{9/2}$–$^6H_{15/2}$. Thus, we can conclude that the environment of the rare-earth ion has rather low symmetry, which is confirmed by the structural analysis data.

In the excitation spectrum of yellow luminescence (Figure 6, curve 1), there is a number of bands associated with the transition from the $^4H_{15/2}$ term to higher energy terms with subsequent relaxation and luminescence from the $^4F_{9/2}$ level. The most intense excitation bands correspond to transitions to the $^4F_{3/2}$, $^4L_{19/2}$ terms; upon excitation to a group of levels with lower energies: $^6P_{5/2}$, $^4M_{19/2}$, $^5F_{7/2}$, $^4I_{13/2}$, luminescence with a lower intensity is observed.

## 4. Conclusions

New $Ln_2Zr(WO_4)_5$ (Ln = Tb, Dy) double tungstates were obtained by ceramic and sol-gel techniques. The conditions of the sol-gel synthesis of tungstates were optimized. Their crystallographic and luminescent properties were determined. It was established that $Ln_2Zr(WO_4)_5$ (Ln= Dy, Tb) double tungstates are crystallized in orthorhombic crystal system, space group $Cmc2_1$ ($Z$ = 4).

The luminescence properties of $Tb^{3+}$, $Dy^{3+}$ ions in tungstate matrices were investigated. The observed spectral lines and bands of luminescence and excitation were identified. The structural features of the considered double tungstates suggest the possibility of their use as matrices for obtaining effective laser materials and promising phosphors.

## Supplementary materials

No supplementary materials are available.

## Funding

This research was carried out within the state assignment of Baikal Institute of Nature Management SB RAS No. 0273-2021-0008.

## Acknowledgment

The Equipment of the Centre for Collective Use of Baikal Institute of Nature Management SB RAS.

## Author contributions

Conceptualization: J.G.B., B.G.B.
Data curation: B.G.B., J.G.B., S.G.D., R.Yu.Sh.
Formal Analysis: S.G.D., D.O.S., Yu.L.T., Ts.T.B., O.D.Ch.
Funding acquisition: J.G.B.
Investigation: S.G.D., D.O.S., R.Yu.Sh.
Methodology: S.G.D., D.O.S., R.Yu.Sh.
Project administration: B.G.B., J.G.B.
Resources: B.G.B., J.G. B., R.Yu.Sh.
Software: S.G.D., D.O.S., R.Yu.Sh.
Supervision: B.G. B., J.G.B.
Validation: S.G. D., D.O. S., R.Yu.Sh.
Visualization: S.G.D., D.O.S., R.Yu.Sh.
Writing – original draft: B.G.B., J.G.B.
Writing – review & editing: S.G.D., D.O.S.

## Conflict of interest

The authors declare no conflict of interest.

## Additional information

Author ID's:
B.G. Bazarov, Scopus ID 7004745799;
S.G. Dorzhieva, Scopus ID 52663542700;
R.Yu. Shendrik, Scopus ID 244020658oo;
Yu.L. Tushinova, Scopus ID 6507295454;
Ts.T. Bazarova, Scopus ID 6603469765;
D.O. Sofich, Scopus ID 57202072039;
O.D. Chimitova, Scopus ID 14059854100;
J.G. Bazarova, Scopus ID 6701747363.

Institute websites:
Baikal Institute of Nature Management SB RAS, https://www.binm.ru/en;
Buryat State University, https://en.bsu.ru;
A.P. Vinogradov Institute of Geochemistry SB RAS, http://www.igc.irk.ru/en;
Irkutsk State University, https://isu.ru/en.

## References

1. Sorokin NI. Ionic conductivity of $KMgCr(MoO_4)_3$ molybdate. Crystallogr Rep. 2017; 62:416–418. doi:10.1134/S106377451703021X
2. Pavlova JeT, Tsyrenova G.D, Lazorjak BI, Solodovnikov SF. The structure and properties of double silver-containing molybdates of the composition $Ag_2A_2(MoO_4)_3$ (A = Mg, Mn, Cu). Vestn Buryats Gos Univ Khim Fiz. 2015;3:3–7. Russian.
3. Savina AA, Solodovnikov SF, Belov DA, Basovich OM, Solodovnikova ZA, Pokholok KV, Stefanovich SYu, Lazoryak BI, Khaikina EG. Synthesis, crystal structure and properties of alluaudite-like triple molybdate $Na_{25}Cs_8Fe_5(MoO_4)_{24}$. J Solid State Chem. 2014;220:217–220. doi:10.1016/j.jssc.2014.09.004
4. Jena P, Nallamuthua N, Patro PK, Venkateswarlu M, Satyanarayana N. Structural characterization and electrical conductivity studies of $BaMoO_4$ nanorods prepared by modified acrylamide assisted sol–gel process. Adv Appl Ceram. 2014;113(6):372–379. doi:10.1179/1743676114Y.0000000170
5. Balsanova LV. Synthesis of crystals of silver-containing oxide phases based on molybdenum, the study of their structure and properties. ESSUTM Bulletin. 2015;5(56):63–69. Russian.
6. Dorzhieva SG, Bazarov BG, Bazarova JG. New molybdates in $Rb_2MoO_4$–$M^I_2MoO_4$–$Zr(MoO_4)_2$ ($M^I$ = Na, K) systems as promis-

ing ion-conducting materials. Lett Mater. 2019;9(1):17–21. doi:10.22226/2410-3535-2019-1-17-21
7. Spiridonova TS, Solodovnikov SF, Savina AA, Kadyrova YM, Solodovnikova ZA, Yudin VN, Stefanovich SY, Khaikina EG. New triple molybdate $Rb_2AgIn(MoO_4)_3$: synthesis, framework crystal structure and ion-transport behavior. Acta Crystallogr C. 2018;74:1603–1609. doi:10.1107/S2053229618014717
8. Lim CS, Aleksandrovsky AS, Molokeev MS, Oreshonkov AS, Ikonnikov DA, Atuchin VV. Triple molybdate scheelite-type upconversion phosphor $NaCaLa(MoO_4)_3$: $Er^{3+}/Yb^{3+}$: structural and spectroscopic properties. Dalton Trans. 2016;45:15541. doi:10.1039/C6DT02378A
9. Dorzhieva SG, Tushinova YL, Bazarov BG, Bazarova ZG, Nepomniashchikh AI, Shendrik RY. Luminescence of Ln-Zr molybdates. Bull Russ Acad Sci Phys. 2015;79(2):276–279. doi:10.7868/S0367676515020076
10. Liao J, Zhou D., Yang B, Liu R, Zhang Q, Zhou QH. Sol-gel preparation and photoluminescence properties of Ca-$La_2(MoO_4)_4$: $Eu^{3+}$ phosphors. J Lumin. 2013;134:533–538. doi:10.1016/j.jlumin.2012.07.033
11. Kozhevnikova NM. Synthesis and luminescence properties of a $Li_3Ba_2La_3(MoO_4)_8$: $Er^{3+}$ phosphor with a scheelite-like structure. Inorg Mater. 2019;55(6):607–611. doi:10.1134/S0002337X19010068
12. Sofich DO, Shendrik RY, Dorzhieva SG, Chimitova OD, Bazarov BG, Tushinova YL, Bazarova ZG. Luminescence of $Pr^{3+}$ and $Nd^{3+}$ ions in double molybdates. Phys Solid State. 2019;61(5):844–846. doi:10.21883/FTT.2019.05.47598.35F
13. Guo C, Yang HK, Jeong JH. Preparation and luminescent properties of phosphor $MgD_2(MoO_4)_4$: $Eu^{3+}$ (M=Ca, Sr, and Ba). J Lumin. 2010;130(8):1390–1393 doi:10.1016/j.jlumin.2010.02.052
14. Liao C, Cao R, Wang W, Hu W, Zheng G., Luo Z, Liu P. Photoluminescence properties and energy transfer of $NaY(MoO_4)_2$: R (R = $Sm^{3+}$ /$Bi^{3+}$, $Tb^{3+}$ /$Bi^{3+}$, $Sm^{3+}$ /$Tb^{3+}$) phosphors. Mater Res Bull. 2018;97:490–496. doi:10.1016/j.materresbull.2017.09.053
15. Song M, Liu Y, Liu Y, Wang L, Zhang N, Wang X, Huang Z, Ji C. Sol-gel synthesis and luminescent properties of a novel $KBaY(MoO_4)_3$: $Dy^{3+}$ phosphor for white light emission. J Lumin. 2019;211:218–226. doi:10.1016/j.jlumin.2019.03.052
16. Grossman VG, Bazarova JG, Molokeev MS, Bazarov BG. New triple molybdate $K_5ScHf(MoO_4)_6$: Synthesis, properties, structure and phase equilibria in the $M_2MoO_4$–$Sc_2(MoO_4)_3$–$Hf(MoO_4)_2$ (M = Li, K) systems. J Solid State Chem. 2020;283:121143. doi:10.1016/j.jssc.2019.121143
17. Bazarova ZhG, Grossman VG, Bazarov BG, Tushinova YuL, Chimitova OD, Bazarova TsT. Phase diagrams for the $M_2MoO_4$-$Ln_2(MoO_4)_3$-$Hf(MoO_4)_2$ systems, where M = Li-Cs, Tl and Ln = La–Lu. Chim Techno Acta. 2017;4(4):224–230. doi:10.15826/chimtech/2017.4.4.03
18. Braziulis G, Janulevicius G, Stankeviciute R, Zalga A. Aqueous sol–gel synthesis and thermoanalytical study of the alkaline earth molybdate precursors. J Therm Anal Calorim. 2014;118:613–621. doi:10.1007/s10973-013-3579-0
19. Bazarov BG, Tsyrendorzhieva AD, Bazarova ZhG, Klevtsova RF, Glinkaja LA, Crystal structure of ternary molybdate $Rb_5FeHf(MoO_4)_6$ – a new phase in the $Rb_2MoO_4$ – $Fe_2(MoO_4)_3$ – $Hf(MoO_4)_2$ system. J Struct Chem. 2004;45(6):993–998. doi:10.1007/s10947-005-0091-9
20. Bazarova JG, Tushinova YuL, Bazarov BG, Dorzhieva SG. Double molybdates of rare earth elements and zirconium. Russ Chem Bull. 2017;66(4):587–592. doi:10.1007/s11172-017-1777-9
21. Klevtsova RF, Solodovnikov SF, Tushinova YL, Bazarov BG, Glinskaya LA, Bazarova ZG. A new type of mixed framework in the crystal structure of binary molybdate $Nd_2Zr_3(MoO_4)_9$. J Struct Chem. 2000;41(2):280–284. doi:10.1007/BF02741593
22. Bazarov BG, Grossman VG, Tushinova YL, Fedorov KN, Bazarova ZG, Klevtsova RF, Glinskaya LA, Anshits AG, Vereshchagina TA. Crystal structure of binary molybdate $Pr_2Hf_3(MoO_4)_9$. J Struct Chem. 2009;50(3):566–569. doi:10.1007/s10947-009-0086-z
23. Grossman VG, Bazarov BG, Bazarova TT, Bazarova JG, Glinskaya LA, Temuujin J. Phase equilibria in the $Tl_2MoO_4$–$Ho_2(MoO_4)_3$–$Zr(MoO_4)_2$ system and the crystal structure of $Ho_2Zr_2(MoO_4)_7$ and $TlHoZr_{0.5}(MoO_4)_4$. J Ceram Process Research. 2017;18(12): 875–881.
24. Bazarov BG, Bazarova JG, Tushinova YL, Solovyov LA, Dorzhieva SG, Surenjav E, Temuujin J. A new double molybdate of erbium and zirconium, its crystalline structure and properties. J Alloys Compd. 2017;701:750–753. doi:10.1016/j.jallcom.2017.01.173
25. Carnall WT, Fields PR, and Rajnak K. J. Chem Phys. 1968;49:4424. doi:10.1063/1.1669893
26. Bazarov BG, Shendrik RYu, Tushinova YL, Sofich DO, Bazarova ZhG. Spectral-luminescent properties of terbium-containing zirconomolybdates. condensed matter and interphases. 2020;22(2):197–203. doi:10.17308/kcmf.2020.22/2831